Catalytic Study of Ethylene Dimerization on Ni(II)-Exchanged Clinoptilolite

Hosun Choo and Larry Kevan*

Department of Chemistry, University of Houston, Houston, Texas 77204-5641

Received: February 22, 2001; In Final Form: April 20, 2001

The catalytic activity and selectivity for ethylene dimerization have been investigated on Ni(II)-exchanged clinoptilolite using a static reactor and gas chromatography. The catalytic results indicate that ethylene is dimerized to *n*-butenes at high temperature via direct reduction of Ni(II) by ethylene in Ni-clinoptilolite containing different cocations. This is consistent with electron spin resonance (ESR) results observed after adsorption of ethylene on Ni(II)-containing clinoptilolite at various reaction temperatures. Our ESR results suggest that Ni(II) in the clinoptilolite structure is reduced by direct interaction with ethylene, leading to the formation of stable Ni(I)-$(C_2D_4)_n$ complexes. At a later stage, several ESR species assigned to Ni(I) complexes with butene are produced as a result of ethylene dimerization. The catalytic performance of Ni-clinoptilolite in ethylene dimerization is dependent on the reaction temperature, the type of cocation and the amount of nickel ions incorporated into extraframework sites of clinoptilolite. Along with *n*-butenes as major products at the initial stage, side products such as methanol, butane, and isobutene increase with reaction time at 623 K. This leads to a decrease in the selectivity for *n*-butene at longer reaction time. The selectivity for *n*-butene is higher at a lower reaction temperature of 523 K, compared to that observed at 623 K, whereas the catalytic activity described as the maximum percent of ethylene converted to *n*-butene is higher at 623 K. This is explained by a higher ESR intensity of Ni(I) species formed at 623 K. Our catalytic results also show similar catalytic activity no matter what type of cocation is present. This is expected by the ESR results showing no large difference in the reducibility of Ni(II) in activated samples containing different cocations. However, the replacement of a smaller cocation with a larger one like Cs^+ increases the selectivity for *n*-butenes. More Ni(II) incorporated into extraframework sites of clinoptilolite increases the formation of *n*-butenes but also causes deactivation more quickly due to reduction of active Ni(I) to inactive Ni(0) by ethylene and butene.

Introduction

It is well-known that nickel ions in zeolites and silicoaluminophosphate (SAPO) materials are active sites for ethylene and propylene dimerization.[1−7] The oligomers produced by this reaction are widely used in the synthesis of detergents or plasticizers, whereas 1-butene, the initial product of ethylene dimerization, is an important comonomer in the production of linear low density polyethylene. It has been suggested that the active site for ethylene dimerization is monovalent Ni(I) formed by reduction of Ni(II) based on observations that the rate of dimerization increased linearly with Ni(I) concentration in photoreduced zeolites and decreased due to further reduction of Ni(I) to Ni(0) by ethylene.[5,8,9] The conversion and selectivity of Ni(II)-modified microporous materials have been mainly affected by the pore size of the framework structure, the location of the nickel ions, and the accessibility of ethylene to the active sites.[10−12]

Clinoptilolite is the most abundant natural zeolite and contains various exchangeable cations to balance the negative charge of the clinoptilolite framework.[13] The framework structure of clinoptilolite, which is isostructural with the zeolite heulandite, is characterized by a two-dimensional channel system.[14,15] This consists of 10-membered ring channels and eight-membered ring channels parallel to each other, which are intersected by other eight-membered ring channels. In the past, papers reporting studies on the catalytic activity of transition-metal-modified zeolites[3,16−18] and SAPO materials[1,2,19] have been published. However, although clinoptilolite is a potential heterogeneous catalyst with a unique framework structure, very few studies have been reported on transition-metal-modified clinoptilolite.[20,21] The main reason seems to be the presence of impurities such as iron and α-quartz in natural clinoptilolite which impurities are very difficult to remove. Furthermore, the difficulties to achieve a reliable synthesis of pure clinoptilolite, which is due to the rather restricted crystallization conditions and gel compositions for successful synthesis of this material,[22,23] delayed extensive catalytic investigation on transition-metal-modified clinoptilolite.

In preliminary work, pure NaK-clinoptilolite was synthesized and characterized by electron spin resonance (ESR) and electron spin echo modulation (ESEM) spectroscopies after Ni(II) was incorporated by ion exchange into extraframework sites.[24] These results indicated the stability and location of active Ni(I) in synthetic clinoptilolite and its coordination with various adsorbates. This information is necessary to understand the catalytic activity of nickel-incorporated clinoptilolite.

As an extension of this work, we describe catalytic studies of ethylene dimerization on Ni(II)-exchanged clinoptilolite. We also report how cocation type, the location and concentration of nickel ion and the reaction temperature affect the catalytic performance of this material for ethylene dimerization. Comparison with similar data for Ni(II)-exchanged mordenite and ferrierite shows the influence of the structural differences of these materials on the catalytic activity for ethylene dimerization.

10.1021/jp0106909 CCC: $20.00
Published on Web 06/08/2001

TABLE 1: Elemental Analysis, Si/Al Ratios and Ni/Al Ratios for NiM-Clinoptilolite (M = Na, K, Ca, and Cs)

catalyst	elemental analysis	Ni(II)/ Al ratio
NiNaK−clino	$Ni_{0.004}Na_{0.057}K_{0.024}\ H_{0.081}[Si_{0.84}Al_{0.17}]O_2$	0.02
NiCaK−clino	$Ni_{0.007}Ca_{0.051}K_{0.010}\ H_{0.095}[Si_{0.84}Al_{0.17}]O_2$	0.04
NiK−clino	$Ni_{0.007}K_{0.099}H_{0.057}[Si_{0.84}Al_{0.17}]O_2$	0.04
NiCsK−clino	$Ni_{0.006}Cs_{0.074}K_{0.036}\ H_{0.048}[Si_{0.84}Al_{0.17}]O_2$	0.04

Experimental Section

Synthesis. The detailed preparation of single phase Na,K-clinoptilolite has been described.[23] Ni(II)M-clinoptilolite (M = Na, K, Ca, and Cs) was prepared as follows. As-synthesized NaK-clinoptilolite was ion-exchanged four times with 1 M MCl (M = Na, K, Ca, and Cs) at 333 K for 24 h. Ni(II) ion was then incorporated into this cocation-containing clinoptilolite by liquid-state ion exchange. Liquid-state ion-exchange was performed by adding 100 mL of 1×10^{-3} M to 1×10^{-1} M $NiCl_2 \cdot 6H_2O$ to 1 g of MK-clinoptilolite (M = Na, K, Ca, and Cs) and stirring overnight at 298 K. The materials were then filtered and washed with hot distilled water to remove the chloride ions. Before and after ion exchange, the sample remained white. The chemical compositions of these various samples were measured by electron microprobe analysis with a JEOL JXA-8600 spectrometer. The results are summarized in Table 1. The amount of protons was calculated based on charge balance with the remaining charge of the framework. Note that significant amounts of potassium ions were still present in the samples even after prolonged ion-exchange with 1 M MCl (M = Na, Ca and Cs) solution. These final ion exchanged samples are designated as NiMK-clinoptilolite (M = Na, Ca, and Cs).

Sample Treatment and Measurement. Powder X-ray diffraction (XRD) patterns were recorded on a Siemens D5000 X-ray diffractometer using Cu Kα radiation.

For ESR and ESEM measurements, hydrated samples were loaded into 3 mm o.d. by 2 mm i.d. Suprasil quartz tubes and were slowly heated under vacuum ($<10^{-4}$ Torr) above room temperature to 623 K for 48 h. This sample was then heated at 623 K in 400 Torr of oxygen for 6 h and subsequently evacuated overnight at the same temperature. This sample is called an "activated" sample containing Ni(II). To stabilize Ni(I), an activated sample was reduced by 100 Torr of hydrogen at 623 K for 1 h. Interaction of Ni(I) with ethylene was investigated by exposure to 20 Torr of C_2D_4 (Cambridge Isotopes) at 298 K for various durations. ESR spectra were recorded at 77 K to detect the formation of any Ni(I) complex with ethylene. To investigate the reduction of Ni(II) by ethylene as a function of temperature, 20 Torr of C_2D_4 (Cambridge Isotopes) was adsorbed on an activated sample containing Ni(II) at 298 K and subsequently heated to various temperatures from 298 to 623 K. These activated samples with ethylene were frozen in liquid nitrogen and sealed for ESR and ESEM measurements.

All ESR spectra were recorded with a Bruker ESP 300 X-band spectrometer at 77 K. The magnetic field was calibrated with a Varian E−500 gaussmeter. The microwave frequency was measured by a Hewlett-Packard HP 5324A frequency counter. ESEM spectra were measured at 5 K with a Bruker ESP 380 pulsed ESR spectrometer. Three pulse echoes were measured by using a $\pi/2-\tau-\pi/2-T-\pi/2$ pulse sequence as a function of time T to obtain a time domain spectrum. The deuterium modulation was analyzed by a spherical approximation for powder samples in terms of N nuclei at distance R with an isotropic hyperfine coupling A_{iso}.[25] The best fit simulation of an ESEM signal is found by varying the parameters until the sum of the squared residuals is minimized.

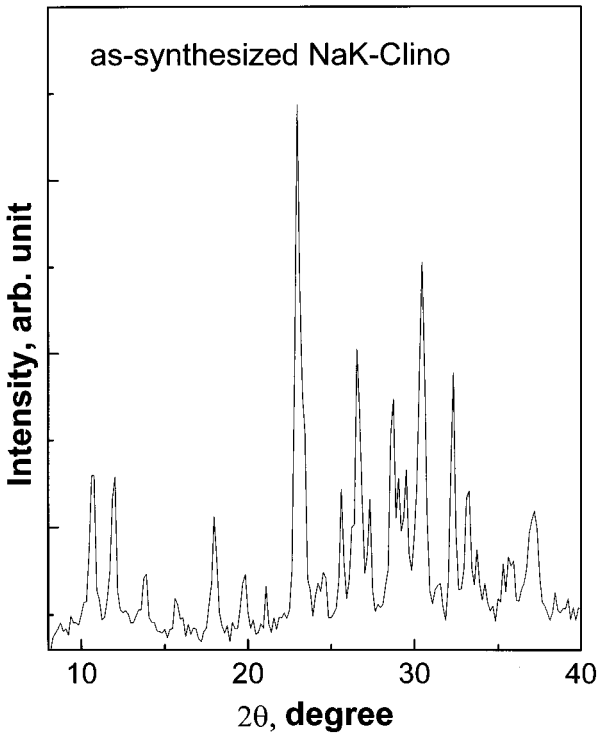

Figure 1. X-ray powder diffraction pattern of as-synthesized NaK-clinoptilolite.

Catalyst Testing. Experments were carried out in a closed, static reactor system. A sample of 100 mg was placed on a sintered glass disk inside a glass reactor of 17 cm^3 total internal volume. The samples activated as described above were exposed to 100 Torr (~0.1 mmol) of ethylene (Trigas) at room temperature and then heated to 523 and 623 K. A gas sample containing ethylene and reaction products was withdrawn from reactor at a specific reaction times and was analyzed by on-line gas chromatography with a Varian 3300 gas chromatograph equipped with a thermal conductivity detector. A 7 ft column of 0.085 inch i.d. packed with 0.19 wt % picric acid supported on a 80/100 mesh graphpac GC support was used. The injection was completed in 5 s.

Results

X-ray Powder Diffraction (XRD). Figure 1 shows the powder XRD pattern of as-synthesized NaK-clinoptilolite. This pattern matches well with the XRD pattern of naturally occurring clinoptilolite.[13]

ESR and ESEM Measurements. Figure 2a shows the ESR spectrum of NiNaK-clinoptilolite after hydrogen reduction at 623 K for 1 h. A sample after activation which includes dehydration, oxidation, and evacuation, gives no ESR signal due to paramagnetic nickel species. However, when 100 Torr of dry hydrogen is adsorbed on Ni(II)NaK-clinoptilolite at 298 K after activation and then this H_2-treated sample is subsequently heated at 623 K for 1 h, two paramagnetic species, denoted A and B. are generated. Species A has axial symmetry with $g_{\parallel}^{A} = 2.445$ and $g_{\perp}^{A} = 2.096$ whereas species B has $g_1^{B} = 2.754$, $g_2^{B} = 2.197$, and $g_3^{B} = 2.024$, indicating lower symmetry of species B. The g values of species A are similar to those reported previously for isolated Ni(I) in NiHSAPO-5, 11, 41,[26−28] and Ni(I)-exchanged X and Y zeolites.[29,30] The symmetry of rhombic species B in NiNaK-clinoptilolite is much lower than that of rhombic Ni(I) species observed in NiNaK-mordenite.[21] These species A and B are assigned to isolated Ni(I) ions located at

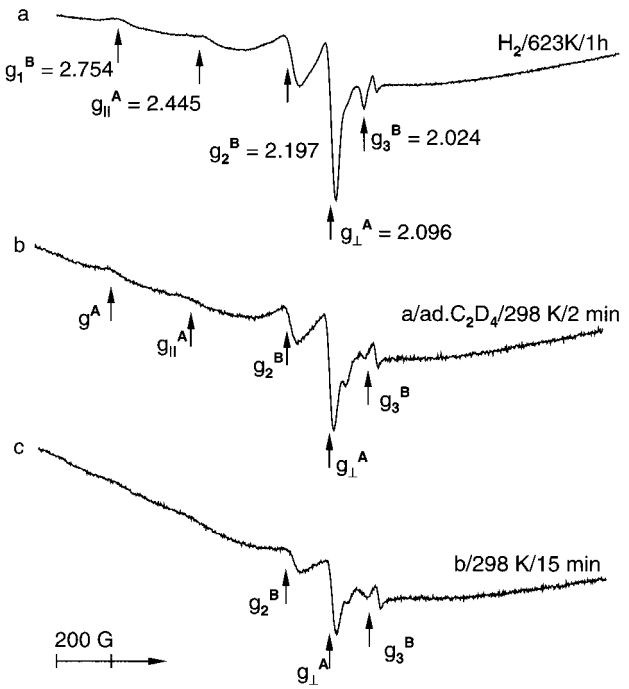

Figure 2. ESR spectra at 77 K of NiNaK-clinoptilolite (a) after hydrogen reduction at 623 K for 1 h and after adsorption of 20 Torr ethylene on a hydrogen-reduced sample at 298 K for (b) 2 min and (c) 15 min.

two different sites within the clinoptilolite structure because they remain unchanged upon evacuation of hydrogen at room temperature. Similar ESR spectra are observed for NiK-, NiCa-, and NiCs-clinoptilolite after hydrogen reduction.

Figure 2b and 2c show the ESR spectra obtained after 20 Torr of ethylene is adsorbed on hydrogen-reduced Ni(I) NaK-clinoptilolite at 298 K for 2 and 15 min, respectively. They do not show any new ESR signal due to the formation of Ni(I) complex with ethylene. The broad baseline seen in NiNaK-clinoptilolite after ethylene adsorption is indicative of the formation of Ni(0) clusters, indicating that Ni(I) species A and B are further reduced to Ni(0) by ethylene. Similar behavior to that of clinoptilolite with respect to ethylene adsorption has been observed in Ni(II)-exchanged H−SAPO-41 where Ni(I) located in a 10-ring channel readily reacts with ethylene and is reduced to Ni(0).[28]

Parts a and b of Figure 3 represent the ESR spectra obtained after 20 Torr of ethylene is adsorbed on activated Ni(II)NaK-clinoptilolite at room temperature which is subsequently heated at 373 and 474 K, respectively, for 1 h. Several paramagnetic ESR species are formed by the interaction of Ni(II) with ethylene at these temperatures. At 373 K, two rhombic species, denoted I and J, are dominant with $g_1^I = 2.615$, $g_2^I = 2.481$, $g_3^I = 1.985$, $g_1^J = 2.718$, $g_2^J = 2.356$, and $g_3^J = 1.971$. Species I and J become more intense without the formation of any new ESR species upon increasing the temperature from 373 to 473 K and to 573 K. These observations suggest that species I and J result from the reduction of Ni(II) to Ni(I) by ethylene at these temperatures and subsequent formation of complexes with ethylene. ESR signals similar to species I have been reported in NiAPSO-5,[31] NiNa−Y,[3] and NiCa-X zeolites[30] after adsorption of ethylene, where they were assigned to Ni(I)−$(C_2D_4)_n$ complexes. Because no new ESR species are observed, even after prolonged annealing time at 373 and 473 K, it is concluded that no dimerization occurs in these systems.

When an ethylene-adsorbed sample is heated at 623 K for 0.5 h, species I and J disappear with the formation of new

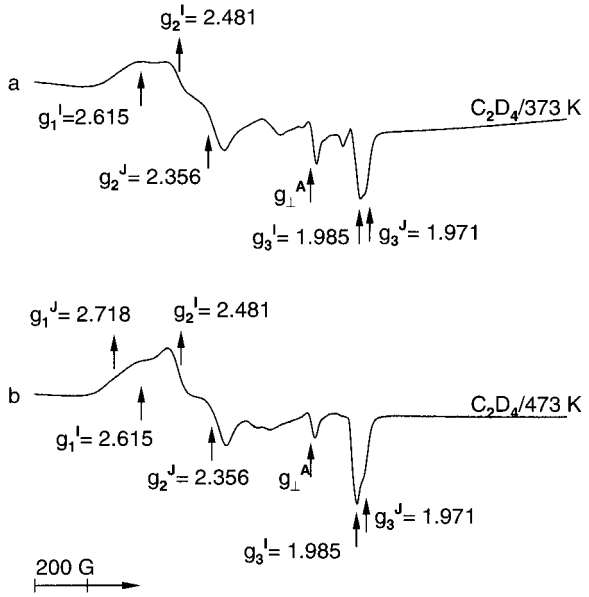

Figure 3. ESR spectra at 77 K of NiNaK-clinoptilolite after 20 Torr of ethylene adsorption at 298 K on an activated sample followed by heating a sample (a) at 373 K for 1 h and (b) at 473 K for 1 h.

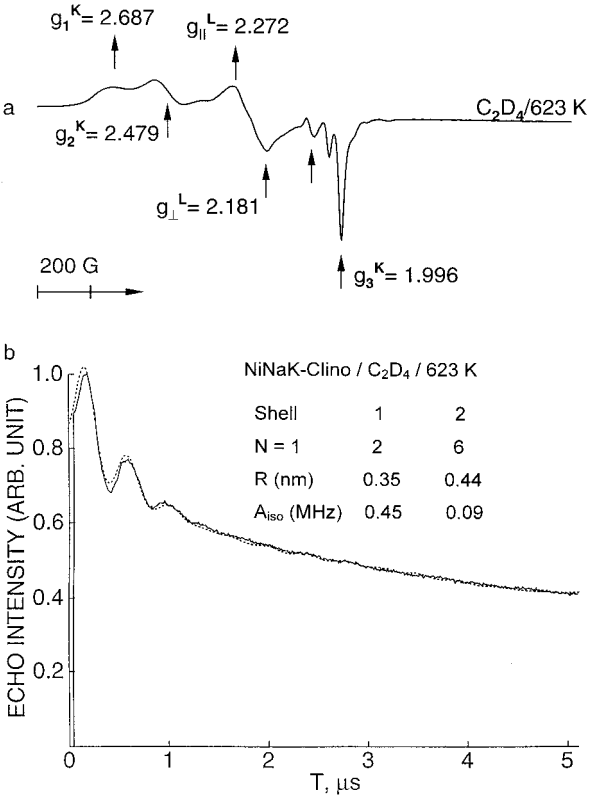

Figure 4. (a) ESR spectrum at 77 K of NiNaK-clinoptilolite after 20 Torr of ethylene adsorption at 298 K on an activated sample followed by heating at 623 K for 30 min and (b) experimental (−−−−) and simulated (- - -) three pulse ^{2}D ESEM spectra at 5 K of NiNaK-clinoptilolite after ethylene adsorption. The spectrum was recorded at the magnetic field corresponding to g_3 of species K.

species K and L as shown in Figure 4a. Species K has $g_1^K = 2.687$, $g_2^K = 2.479$, and $g_3^K = 1.996$ and is assigned to a Ni(I) complex with butene, the product of ethylene dimerization. This assignment is confirmed by ESEM data. Figure 4b shows the experimental and simulated three-pulse deuterium ESEM spectra for species K. The best fit simulation gives two deuterium nuclei at a distance of 0.35 nm and another six nuclei at a distance of

TABLE 2: ESR *g* Values of Paramagnetic Species Produced after Adsorption of Ethylene on Ni(II)NaK−Clinoptilolite under Various Reaction Conditions

reaction temp (K)	adsorbate	assignment	$g_{\|\|}$ or g_1	$g_\perp$ or g_2	g_3	species
623	H_2	Ni(I)	2.445	2.096		A
623	H_2	Ni(I)	2.754	2.197	2.024	B
< 623	C_2D_4	Ni(I)−$(C_2D_4)_n$	2.615	2.481	1.985	I
< 623	C_2D_4	Ni(I)−$(C_2D_4)_n$	2.718	2.356	1.971	J
623	C_2D_4	Ni(I)−$(C_4D_8)_1$	2.687	2.479	1.996	K
623	C_2D_4	Ni(I)−$(C_4D_8)_n$	2.272	2.181		L

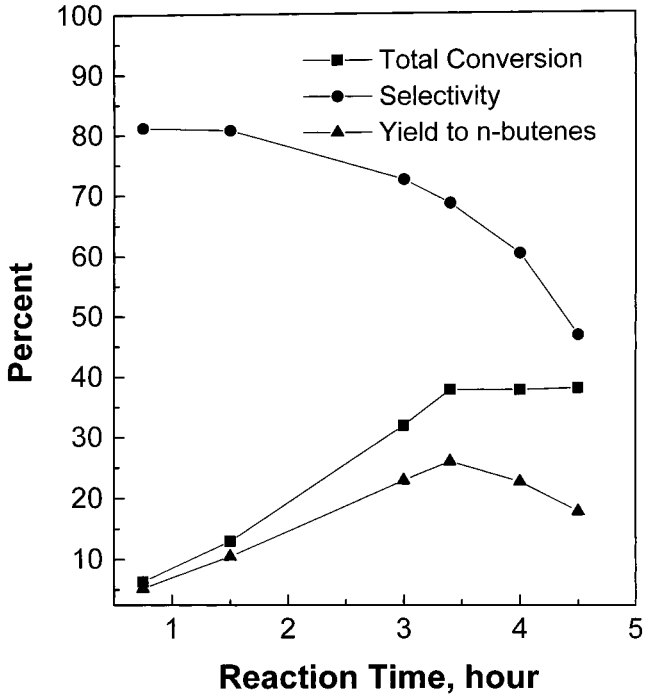

Figure 5. Total conversion (%) of ethylene, the selectivity (%) to *n*-butenes and the yield (%) of *n*-butenes over activated NiNaK-clinoptilolite at 623 K as a function of reaction time.

0.44 nm, confirming the formation of a Ni(I)−$(C_4D_8)_1$ complex as a result of ethylene dimerization. Species L with $g_{\|}^L = 2.272$ and $g_\perp^L = 2.181$ is probably due to another Ni(I) complex with butene because this species appears along with species K, a Ni(I)−$(C_4D_8)_1$ complex, only at a higher temperature.

Table 2 summarizes the ESR parameters of Ni(I) species observed after adsorption of ethylene on NiNaK-clinoptilolite under various reaction conditions.

Catalyst Testing. Dehydrated MK-clinoptilolite (M = Na, Ca, K, and Cs) shows no ethylene dimerization activity under the reaction condition. However, Ni(II)-exchanged MK-clinoptilolite (M = Na, Cs, K, and Cs) is active for ethylene dimerization when the activated sample is exposed to 100 Torr of ethylene at 298 K and is subsequently heated at 623 K for various durations. Although proton-exchanged clinoptilolite (HK-clinoptilolite) not containing Ni(II) ions shows catalytic activity for ethylene dimerization under the same conditons, the percentage yield of *n*-butene is much lower (3%) compared to the yields observed in Ni(II)-exchanged clinoptilolite samples. This indicates that nickel ions directly participate in the formation of catalytically active sites. Table 1 shows the chemical composition of the samples used for the catalytic runs of ethylene dimerization.

Figure 5 shows the total conversion of ethylene, the selectivity to *n*-butenes and the yield of *n*-butenes over activated NiNaK-clinoptilolite at 623 K as a function of reaction time. In addition

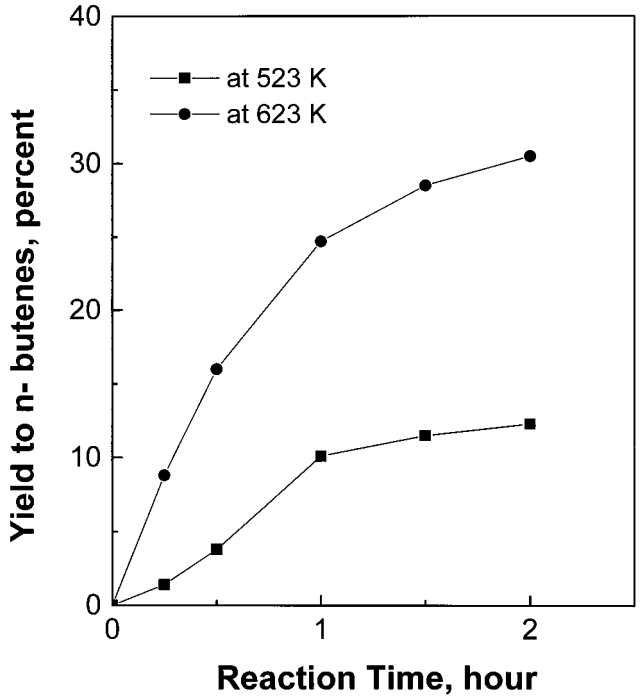

Figure 6. Yield (%) of *n*-butenes produced from ethylene at two different reaction temperatures, 523 and 623 K, as a function of reaction time.

to 1-butene, *cis*-, and *trans*-2-butene, which are the main products at the initial stage; propylene, isobutane, isobutene and methane are also detected as side products and they become dominant with longer reaction time. For the calculation of percent yield, the three isomers of *n*-butene are grouped together. The total conversion of ethylene increases from 6.3% at 45 min reaction time to 38% at 3.5 h and then reaches a plateau, whereas the selectivity to *n*-butene continuously decreases with reaction time, as seen in Figure 5. It is clear that a difference in percent between the total conversion of ethylene and the yield of *n*-butene increases with reaction time, leading to a decrease in the selectivity to *n*-butene as a function of reaction time. This is explained by the fact that a portion of the side products such as methane and isobutane increase as the reaction time increases at 623 K. This is probably due to isomerization of butene followed by cracking at this high temperature. The catalysts turned brown and later dark gray during the reaction.

Figure 6 shows the percent yield of *n*-butene produced at two different reaction temperatures, 523 and 623 K, as a function of reaction time for NiNaK-clinoptilolite. Formation of *n*-butenes is much faster at 623 K as indicated in its higher initial rate for the formation of *n*-butenes at 623 K compared to that observed at 523 K. In contrast, the selectivity to *n*-butenes is much lower at 623 K. A NiNaK-clinoptilolite catalyst exhibits almost 100% selectivity to *n*-butenes at 523 K throughout the reaction time range. The selectivity for NiNaK-clinoptilolite at 623 K is 94.3% at 0.5 h reaction time and continuously drops with longer reaction time. This indicates that the isomerization and cracking of *n*-butenes, which produce side products such as isobutene, isobutane, and methane, are associated with high temperatures. It has been reported that ethylene is initially dimerized to 1-butene, which is subsequently isomerized to *cis*-2-butene and *trans*-2-butene.[32] Analysis of the gas phase during the catalytic reaction of clinoptilolite at 623 K indicates that the *cis*-/*trans*-2-butene ratio, at a reaction time of 15 min, is close to the thermal equilibrium value and the composition of butene isomers does not change appreciably with reaction time. These observa-

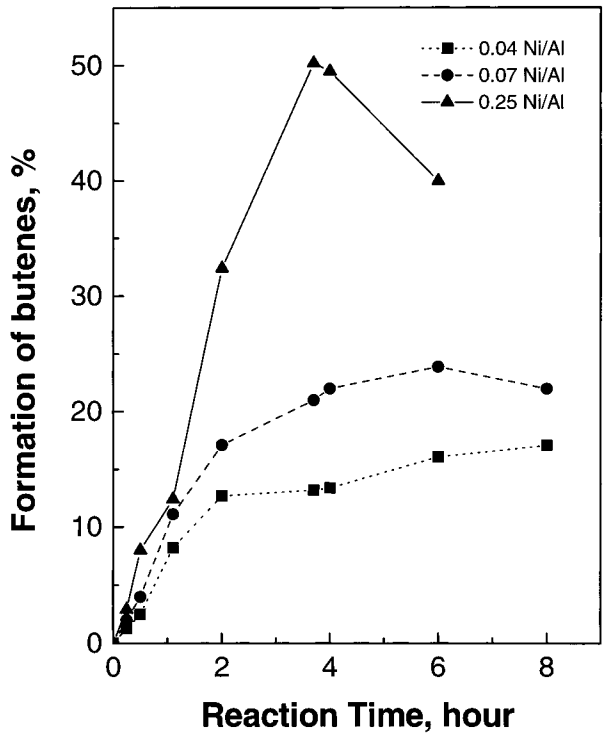

Figure 7. Yield (%) of *n*-butenes from ethylene as a function of time at 623 K for NiNaK-clinoptilolite with Ni/Al = 0.04, 0.07 and 0.25.

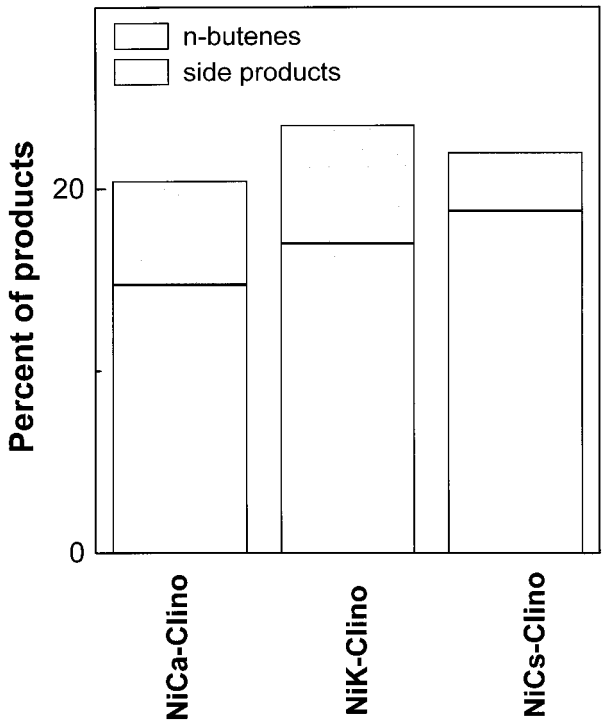

Figure 8. Distribution between *n*-butenes and side products in the gas phase after a 6 h reaction period at 623 K in NiCaK-clinoptilolite, NiK-clinoptilolite, and NiCsK-clinoptilolite.

tions suggest that *n*-butenes formed in NiNaK-clinoptilolite reach equilibrium rapidly at a reaction temperature of 623 K.

The influence of Ni(II) concentration on the catalytic activity of ethylene dimerization is studied for NiNaK-clinoptilolite at 623 K. Figure 7 represents the percent yield of *n*-butene as a function of reaction time for three NiNaK-clinoptilolite samples showing different Ni(II)/Al ratios, 0.04, 0.07, and 0.25, respectively, based on electron microprobe analysis. It is observed that an increase in the Ni(II) concentration increases the catalytic activity described as the maximum percentage of ethylene converted to *n*-butenes. The initial rate for the formation of *n*-butenes also increases with the concentration of Ni(II) incorporated. This is evident from the initial slope of the line shown in Figure 7. For the catalyst with lowest nickel concentration (Ni(II)/Al = 0.04), the yield of *n*-butenes increases continuously throughout the reaction time range employed and reaches a maximum of 17% at a reaction time of 8 h. Upon increasing the concentration of Ni (Ni(II)/Al = 0.07), the catalytic activity for the formation of *n*-butenes increases with a higher initial rate. It reaches a maximum yield of ~24%, at a reaction temperature of 6 h and then starts to decrease slowly. In contrast, for NiNaK-clinoptilolite containing the highest Ni(II) amount (Ni(II)/Al = 0.25), the conversion of ethylene to *n*-butenes sharply increases to reach a maximum (~50%) at a reaction time of ~4 h and then decreases rapidly to reach ~40% at a 6 h reaction time, which is 20% lower than the maximum yield.

Figure 8 shows the influence of cocations on the distribution between *n*-butenes and side products in the gas phase after a 6 h reaction period at 623 K for NiCaK-clinoptilolite, NiK-clinoptilolite, and NiCsK-clinoptilolite with the same nickel(II) concentration but with different major cocations. There is no large difference in the catalytic activity of ethylene dimerization between these three samples. This observation is consistent with ESR results indicating no difference in the reducibility of Ni(II) in Ni-clinoptilolite containing different sizes of cocations. However, the selectivity toward *n*-butenes is different depending on the type of major cocation present. It is clear from Figure 8 that NiCsK-clinoptilolite exhibits the highest selectivity toward *n*-butene compared to those of NiK-clinoptilolite and NiCaK-clinoptilolite.

TABLE 3: Ethylene Dimerization on Activated Ni(II)NaK−Clinoptilolite and on Reduced Ni(I)NaK−Clinoptilolite, Ni(I)NaK−Ferrierite, and Ni(I)NaK−Mordenite

catalyst	Ni(II)/ Al ratio	reaction temp (K)	yield %	initial rate (mmol/h/g)
Ni(II)NaK−clino	0.04	623	17	5.5
Ni(II)NaK−clino	0.07	623	24	10
Ni(II)NaK−clino	0.25	623	50	17
Ni(II)NaK−clino	0.25	523	-	4.8
Ni(II)CaK−clino	0.04	623	15	
Ni(II)K−clino	0.04	623	17	
Ni(II)CsK−clino	0.04	623	19	
Ni(I)NaK−clino	0.04	298	0	
Ni(I)NaK−fer	0.04	298	2.0	
Ni(I)NaK−mor	0.03	298	0.12	

Table 3 summarizes the catalytic results for ethylene dimerization on NiNaK-clinoptilolite compared with those observed on NiNaK-mordenite[33] and NiNaK-ferrierite.[33]

Discussion

Clinoptilolite is a medium pore zeolite whose framework is composed of alternating SiO_4 and AlO_4 tetrahedra with a Si/Al ratio of 4.9.[13−15] These units are linked together to form a two-dimensional channel structure with elliptical pore openings. A structural model of clinoptilolite is shown in Figure 9. The 10-membered channel and one eight-membered channel run side by side along the *c*-axis. They are intersected by another eight-membered channel that runs along the *a*-axis. Because of the excess negative charge present on the AlO_2 units, compensating cations, mainly potassium and sodium, are present to balance the charge in the zeolite framework.

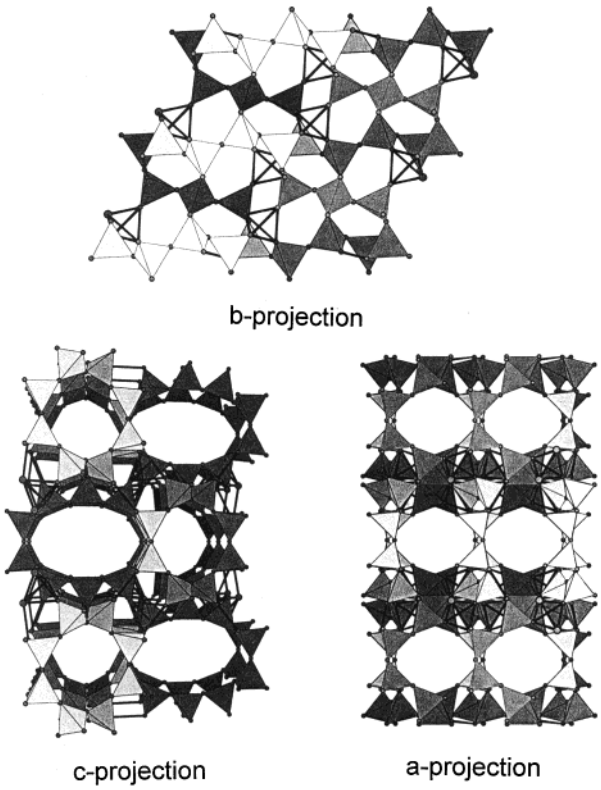

Figure 9. Structural model of clinoptilolite. The corner of a tetrahedron represents framework oxygen. Al and Si atoms are located at the centers of the tetrahedra.

Hydrogen reduction of NiNaK-clinoptilolite produces two paramagnetic Ni(I) species, denoted as A and B, which result from reduction of Ni(II) to Ni(I) by hydrogen at 623 K. Species A has axial symmetry, whereas species B has rhombic symmetry based on their g anisotropies. Both species A and B are assigned to isolated Ni(I) ions situated at two different sites of clinoptilolite because these species remain upon evacuation of hydrogen at 298 K. Isolated axial symmetric Ni(I) species with the ESR parameters similar to those of Ni(I) species A have been observed in NiNaK-ferrierite[21] and SAPO materials[26−28] after thermal and hydrogen reduction at high temperatures. The higher reducibility of Ni(II) observed in NiNaK-ferrierite compared to that in NiNaK-clinoptilolite after hydrogen reduction under the same conditions is mainly ascribed to the lesser negative charge of the ferrierite framework as shown by the higher Si/Al ratio of ferrierite. Hydrogen reduction of NiNaK-mordenite[21] also produced single isolated Ni(I) showing rhombic symmetry but the g parameters of this Ni(I) are much smaller than those of rhombic Ni(I) species B observed in NiNaK-clinoptilolite.

Adsorption of ethylene on hydrogen-reduced Ni(I)NaK-clinoptilolite at 298 K leads to a broad ESR signal associated with the formation of Ni(0) clusters, suggesting that Ni(I) species A and B in clinoptilolite are further reduced to Ni(0) by ethylene. The baseline shows more broadening as the annealing time increases at 298 K. This behavior of Ni(I) in clinoptilolite with respect to adsorption of ethylene at room temperature is different from the behavior observed in NiNaK-ferrierite,[21] NiNaK-mordenite[21] and nickel-exchanged SAPO materials[2,19] where Ni(I) ions initially coordinated with ethylene to form stable Ni(I)-$(C_2H_4)_n$ complexes. In SAPO materials, Ni(I)−$(C_4H_8)_n$ complexes were observed as a result of ethylene dimerization when a sample with adsorbed ethylene was annealed at 298 or 353 K for a longer time.[1,2,19]

The formation of *n*-butenes, the products of ethylene dimerization, in clinoptilolite is achieved in the different way compared to that observed in nickel-exchanged NiNaK-ferrierite,[21] NiNaK-mordenite,[21] and nickel-exchanged SAPO materials.[1,2,19] No ESR species due to Ni(I) complexes with ethylene and butene produced as a result of ethylene dimerization are observed without heating activated Ni(II)NaK-clinoptilolite after ethylene adsorption at room temperature. The formation of stable Ni(I) complexes with ethylene or butene at 623 K can be explained by direct reduction of Ni(II) by ethylene followed by subsequent formation of complexes. Unlike NiNaK-clinoptilolite, the direct reduction of Ni(II) by ethylene at high temperatures in NiNaK-mordenite and NiNaK-ferrierite immediately leads to the formation of Ni(0) clusters without forming any Ni(I) complex with ethylene or butene.[33] This indicates that the reduction of Ni(II) occurs more rapidly in NiNaK-mordenite and NiNaK-ferrierite than in NiNaK-clinoptilolite. This reflects the different environments of Ni(I) and Ni(II) ions between NiNaK-mordenite, NiNaK-ferrierite, and NiNaK-clinoptilolite. The exact mechansim by which Ni(I) is generated during the interaction of Ni(II) with ethylene at high temperature is unknown. However, the observation of ESR species assigned to Ni(I) complexes with ethylene suggest the formation of Ni(I)—$(C_2H_4)^+$.

The simulation of the ^{2}D ESEM spectrum obtained for Ni(I)-butene species K shows that a Ni(I) ion interacts with one C_4D_8 molecule where two deuteriums are closer to Ni(I) than the other six deuteriums. Note that there are three butene isomers with different geometries. Our ESEM analysis somewhat reflects that this species K is due to a Ni(I) complex with cis or *trans*-2-butene because assuming a π-bonding interaction between Ni(I) and one butene molecule, two deuteriums (*cis*/*trans*-2-butene) or three deuteriums (1-butene) should be closer to Ni(I) than the other deuteriums. Similar simulation parameters have been observed for Ni(I)-butene complexes in SAPO-5, 11, and MCM-41.[1,2,34]

As already expected by the ESR and ESEM results, our catalytic results show that ethylene dimerization occurs on this nickel-exchanged clinoptilolite during the reduction of an activated sample containing Ni(II) at 623 K. The total conversion of ethylene increases at 623 K, whereas the selectivity decreases with longer reaction time. Along with an initial ethylene dimerization product, 1-butene, side products such as *n*-butenes, isobutene, propylene, isobutane, and methane are generated at longer reaction time due to side reactions. The 1-butene isomerization reactions followed by cracking become profound for a longer annealing time at 623 K. This trend is evident from an increase in the percent difference between total conversion and the yield of *n*-butenes as is seen in Figure 5.

The catalytic activity and selectivity for ethylene dimerization have been investigated previously for other microporous materials such as X and Y zeolites,[3,9] ferrierite, mordenite[33] and SAPO materials[1,2,9] with different channel dimensions. As mentioned earlier, the experimental procedure used in these materials for the formation of *n*-butene is completely different from that employed in clinoptilolite. Ethylene was selectively dimerized to *n*-butenes in these materials when ethylene-adsorbed samples are annealed at 298 or 353 K only after active Ni(I) sites are prepared by thermal or hydrogen reduction of these Ni(II)-containing materials. The observation that these materials not containing nickel ions show no catalytic activity for ethylene dimerization suggests that Ni(I) is the catalytically active site for ethylene dimerization. For Ni-clinoptilolite, active Ni(I) sites are prepared via direct reduction of Ni(II) by ethylene at the

temperatures higher than 373 K. It has been reported that ethylene is initially dimerized to 1-butene, which is subsequently isomerized to *cis*- and *trans*-2-butene mainly on acid sites to reach the thermal equilibrium distribution of these butene isomers.[32] Analysis of the composition of the butene products indicates that *n*-butenes attain a thermal equilibrium distribution rapidly at an early stage of reaction. This is probably due to the large interconnecting channel system in clinoptilolite where *n*-butene products easily diffuse to acid sites in the clinoptilolite framework.

The catalytic activity of NiNaK-clinoptilolite for ethylene dimerization is affected by the reaction temperature, the type of cocation and the amount of nickel ions incorporated into the extraframework sites of clinoptilolite. Decreasing the reaction temperature enhances the selectivity of NiNaK-clinoptilolite for *n*-butenes. However, the initial rate for the formation of *n*-butene and the catalytic activity described as the maximum percent of ethylene converted to *n*-butenes is much higher at 623 K compared to 523 K. This is explained by the ESR results showing that the reducibility of Ni(II) in clinoptilolite increases at the higher reduction temperature of 623 K. Another possible reason is that the formation of side products seems to be closely associated with high temperature. H-clinoptilolite has been found to be highly active for 1-butene isomerization at reaction temperatures higher that 573 K.[35,36] The main products besides the *n*-butenes were isobutenes and several cracking products. Our results suggest that higher temperature favors the formation of *n*-butenes as well as side products.

The amount of Ni(II) incorporated into the extraframework sites of clinoptilolite influences its catalytic performance for ethylene dimerization. The initial rate and catalytic activity for the formation of *n*-butenes increase with the Ni(II) concentration in NiNaK-clinoptilolite. As the Ni concentration increases, the catalyst quickly reaches its maximum activity as well as shows fast deactivation. This is probably due to the fact that reduction of Ni(II) to Ni(I) at high temperature is accompanied by the formation of Ni(0) clusters which are catalytically inactive. This deactivation process becomes more rapid as the Ni concentration and reaction temperature increase.

It is quite apparent from our experimental results that Cs substitution into an extraframework site of clinoptilolite increases its selectivity toward *n*-butene by comparing the selectivity of *n*-butene among clinoptilolite materials containing the same amount of Ni(II) but having different sizes of cocations such as Ca, K, and Cs. A major factor which influences the selectivity for *n*-butenes in channel-type zeolites and SAPO materials is the main channel size.[1,35] For instance, the selectivity for the formation of *n*-butenes is higher in SAPO-11 than SAPO-5. SAPO-11 has a smaller channel which allows efficient production of *n*-butenes but suppresses side reactions, whereas SAPO-5 has a larger channel which allows more side reactions.[1,2] Similarly, the replacement of smaller ions like K^+ and Ca^{2+} with larger ions like Cs^+ limits the diffusion of *n*-butene side products. This unique behavior of clinoptilolite is a consequence of its structure.

Conclusions

This work investigates the catalytic activity and selectivity for ethylene dimerization in Ni(II)-exchanged clinoptilolite. The catalytic results are correlated to ESR results observed after adsorption of ethylene on Ni(II)-containing clinoptilolite at various reaction temperatures. The ESR and catalytic results indicate that ethylene is dimerized to *n*-butenes at high temperature via direct reduction of Ni(II) by ethylene in Ni-clinoptilolite containing different cocations. Adsorption of ethylene on reduced Ni(I)-clinoptilolite at 298 K leads to the formation of Ni(0) clusters without forming any Ni(I) complexes with ethylene or butene. This indicates that further reduction of Ni(I) occurs by ethylene and no ethylene dimerization occurs.

The reaction temperature, the type of cocation and the amount of nickel ions incorporated into extraframework sites of clinoptilolite affect the catalytic performance of NiNaK-clinoptilolite for ethylene dimerization. The formation of *n*-butenes increases to a maximum and then decreases at a reaction temperature of 623 K. Along with the *n*-butene major products, side products such as methanol, butane and isobutene increase with reaction time at 623 K, leading to a decrease in the selectivity for *n*-butene at longer reaction time. The selectivity for *n*-butene is higher at a lower reaction temperature of 523 K compared to 623 K, whereas the catalytic activity is higher at 623 K. Our catalytic results also show similar catalytic activity for different cocations as expected from the ESR results showing no large difference in the reducibility of Ni(II) in clinoptilolite containing different cocations. But the replacement of smaller cocations with a large one like Cs^+ enhances the selectivity for *n*-butenes. The formation of *n*-butenes increases with the amount of Ni(II), but greater Ni(II) also causes faster deactivation due to formation of inactive Ni(0) clusters.

Acknowledgment. This research was supported by the National Science Foundation, the Robert A. Welch Foundation and the Environmental Institute of Houston.

References and Notes

(1) Hartmann, M.; Kevan, L. *J. Chem. Soc., Faraday Trans.* **1996**, *92*, 1429.
(2) Hartmann, M.; Kevan, L. In *Progress in Zeolite and Microporous Material*; Chon, H., Ihm, S. K., Uh, Y. S., Eds.; Surface Science and Catalysis, Vol 105A; Elsevier: New York, 1997; pp 717−724.
(3) Ghosh, A. K.; Kevan, L. *J. Phys. Chem. B* **1990**, *94*, 3117.
(4) Elev, I. V.; Shelimov, B. N.; Kazansky, V. B. *J. Mol. Catal*. **1983**, *21*, 265.
(5) Elev, I. V.; Shelimov, B. N.; Kazansky, V. B. *J. Catal*. **1984**, *89*, 470.
(6) Maruja, K.; Ozaki, A. *Bull. Chem. Soc. Jpn.* **1973**, *46*, 351.
(7) Yashima, T.; Ushida, Y.; Ebisawa, M.; Hara, N. *J. Catal*. **1975**, *36*, 320.
(8) Schmidt, F. K.; Mironova, L. V.; Saraev, V. V.; Gruznych, V. A.; Dmitrieva, T. V. Ratovsky, G. *Kinet. Katal.* **1979**, *20*, 622.
(9) Bonneviot, L.; Oliver, D.; Che, M. *J. Mol. Catal.* **1983**, *21*, 415.
(10) Smith, J. V. In *Zeolite Chemistry and Catalysis*; Rabo, J. A., Ed.; American Chemical Society: Washington, DC, 1976; Chapter 1.
(11) Ben Tarrit, Y.; Che, M. In *Catalysis by Zeolites*; Imelik, B., Naccache, C., Ben Taarit, Y., Vedrine, J. C., Coudurier, G., Pratiaud, H., Eds.; Elsevier: Amsterdam, 1980; p 167.
(12) Maxwell, I. E. *Adv. Catal.* **1982**, *31*, 1.
(13) Gottardi, G.; Galli, E. *Natural Zeolites*; Springer-Verlag: Berlin, 1985; p 256.
(14) Koyama, K.; Takeuchi, Y. Z. *Kristallogr*. **1997**, *145*, 216.
(15) Smyth, J. R.; Sapid, A. T. *Am. Mineral.* **1990**, *75*, 522.
(16) Sachtler, W. M. H.; Zhang, Z. *Adv. Catal*. **1993**, *39*, 129.
(17) Shelef, M. *Chem. Rev*. **1995**, *95*, 209.
(18) Minachev, Kh. M.; Garanin, V. I.; Kharlamov, V. V.; Isakova, T. A. *Kinet. Katal.* **1972**, *13*, 1101.
(19) Hartmann, M.; Kevan, L. *J. Phys. Chem. B* **1996**, *100*, 4606.
(20) Kim, Y. G.; Kim, Y. C.; Hong, S. B.; Kim, M. H.; Kim, Y. P.; Uh, Y. S. *Catal. Lett.* **1999**, *57*, 179.
(21) Choo, H.; Hong, S. B.; Kevan, L. *J. Phys. Chem. B.* **2001**, *105*, 0000.
(22) Williams, C. D. *J. Chem. Soc., Chem. Commun*. **1997**, 2113.
(23) Zhao, D.; Szostak, R.; Kevan, L. *The Energy Lab Electronic Newsletter* **1997**, *34*, 5.
(24) Choo, H.; Prakash, A. M.; Park, S. K.; Kevan, L. *J. Phys. Chem. B* **1999**, *103*, 6193.
(25) Kevan, L. In *Time Domain Electron Spin Resonance*; Kevan, L., Schwartz, R. N., Eds.; Wiley: New York, 1979; Chapter 8.
(26) Azuma, N.; Hartmann, M.; Kevan, L. *J. Phys. Chem.* **1995**, *99*, 6670.

(27) Azuma, N.; Lee, C. W.; Kevan, L. *J. Phys. Chem.* **1994**, *99*, 1217.
(28) Prakash, A. M.; Wasowicz, T.; Kevan, L. *J. Phys. Chem.* **1997**, *101*, 1985.
(29) Schoonheydt, R.; Roodhooft, D. *J. Phys. Chem.* **1986**, *90*, 6319.
(30) Michalik, J.; Narayama, M.; Kevan, L. *J. Phys. Chem.* **1984**, *88*, 5236.
(31) Hartmann, M.; Azuma, N.; Kevan, L. *J. Phys. Chem.* **1995**, *99*, 10 988.
(32) Sohn, J. R.; Shin, D. C. *J. Catal.* **1996**, *160*, 314.
(33) Choo, H.; Kevan, L., unpublished results.
(34) Hartmann, M.; Poppl, A.; Kevan, L. *J. Phys. Chem.* **1996**, *100*, 9906.
(35) Woo, H. C.; Lee, K. H.; Lee, J. S. *Appl. Catal*. **1996**, *134*, 147.
(36) Seo, G.; Kim, M. W.; Kim, J. H.; Ahn, B. J.; Hong, S. B.; Uh, Y. S. *Catal. Lett.* **1998**, *55*, 105.